Fermion dark matter at the center and in the halo of the Galaxy

Neven Bilić‡ , Sam Halliday, Gary B. Tupper and Raoul D. Viollier§
Institute of Theoretical Physics and Astrophysics,
Department of Physics, University of Cape Town,
Private Bag, Rondebosch 7701, South Africa

Abstract. After a discussion of the properties of degenerate fermion balls, we analyze the orbits of the star S0-2, in the supermassive black hole as well as in the fermion ball scenarios of the Galactic center. It is shown that both scenarios are consistent with the data of S0-2, which since 1992 has had a projected distance to Sgr A* smaller than 10 light-days, as measured during eight years by Eckart *et al.* and Ghez *et al.* The free parameters of the projected orbit of a star are the unknown components of its velocity v_z and distance z to Sgr A* in 1992.7 with the z-axis being in the line of sight. We show that the $v_z - z$ phase space, which fits the data of S0-2, is much larger in the fermion ball than in the black hole scenario. Future measurements of the projected and radial positions and velocities of S0-1 and S0-2, which both could be orbiting within such a fermion ball of $2.6 \times 10^6 M_\odot$ mass and 21 light-days radius, may reduce this allowed phase space, eventually ruling out one of the currently acceptable scenarios. This could shed some light on the nature of the supermassive compact dark object, or dark matter in general, at the center of our Galaxy. We then consider a self-gravitating ideal fermion gas at nonzero temperature as a model for the Galactic halo. The Galactic halo of mass $\sim 2 \times 10^{12} M_\odot$, enclosed within a radius of $\sim$ 200 kpc, is consistent with the existence of a supermassive compact dark object at the Galactic center that is in hydrostatic and quasi-thermal equilibrium with the halo. The central object has a maximal mass of $\sim 2.3 \times 10^6 M_\odot$ within a minimal radius of $\sim$ 18 mpc or $\sim$ 21 light-days for fermion masses $\sim$ 15 keV. We thus conclude that both the supermassive compact dark object and the halo could be made of the same nearly non-interacting $\sim$ 15 keV fermion.

1. Introduction

Self-gravitating degenerate matter was suggested as a model for quasars, with neutrino masses in the $0.2\ \mathrm{keV} \lesssim m \lesssim 0.5\ \mathrm{MeV}$ range [1], many years prior to the inception of the black hole hypothesis [2]. More recently, supermassive compact dark objects consisting of nearly non-interacting degenerate fermionic matter, with fermion masses in the $10 \lesssim m/\mathrm{keV} \lesssim 20$ range, have been proposed [3, 4, 5, 6, 7] as an alternative to supermassive black holes, which are believed to reside at the centers of many active and inactive galaxies.

The masses of ~ 20 supermassive compact dark objects at the centers of inactive galaxies [8] have been measured so far. The most massive compact dark object ever observed is located at the center of M87 in the Virgo cluster, and has a mass of $\sim 3 \times 10^9 M_\odot$ [9]. If we identify this object of maximal mass with a degenerate fermion ball at the Oppenheimer-Volkoff (OV) limit [10], i.e. $M_{\mathrm{OV}} = 0.54\, M_{\mathrm{Pl}}^3 m^{-2} g^{-1/2} \simeq 3 \times 10^9 M_\odot$ [5], where $M_{\mathrm{Pl}} = \sqrt{\hbar c/G}$ is the Planck mass, this allows us to fix the fermion mass to $m \simeq$ 15 keV for a spin and particle-antiparticle degeneracy factor $g = 2$. Such a relativistic object would have a radius

‡ Permanent address: Rudjer Bošković Institute, P.O. Box 180, 10002 Zagreb, Croatia; Email: bilic@thphys.irb.hr
§ Email: viollier@physci.uct.ac.za

$R_{\rm OV} = 4.45\ R_{\rm S}(M_{\rm OV}) \simeq 1.5$ light-days (ld), where $R_{\rm S}(M_{\rm OV})$ is the Schwarzschild radius of the mass $M_{\rm OV}$. It would be virtually indistinguishable from a black hole of the same mass, as the closest stable orbit around such a black hole has a radius of 3 $R_{\rm S}(M_{\rm OV})$.

At the lower end of the observed mass range is the compact dark object located at the center of our Galaxy [11], having a mass $M_{\rm c} \simeq 2.6 \times 10^6 M_\odot$. Interpreting this object as a degenerate fermion ball consisting of the same $m \simeq 15$ keV and $g = 2$ fermions, the radius is $R_{\rm c} \simeq 21$ ld $\simeq 7 \times 10^4 R_{\rm S}(M_c)$ [3]. Such a nonrelativistic object is far from being a black hole. The observed motion of stars within a projected distance of ~ 50 ld from Sgr A* [11], the powerful and enigmatic radio source at the Galactic center, yields, apart from the mass, a conservative upper limit for the radius of the fermion ball, $R_{\rm c} \lesssim 21$ ld. Matter orbiting in an optically thick and geometrically thin accretion disk in or around such a fermion ball would only radiate at distances $\gtrsim$ 12 ld from the center, as both the density and the circular frequency become nearly constant near the center of the fermion ball [6]. In contrast to the black hole scenario, the spectrum emitted by the disk in and around a fermion ball will thus have a cut-off at frequencies $\gtrsim 10^{13}$ Hz, as is actually observed. Since the accreting matter is unable to radiate off its energy, it cannot spiral inward any further, leading presumably to a pile-up of baryonic matter at $\sim$ 12 ld from the center. Gravitational instabilities may result in the formation of massive stars at a rate corresponding to the accretion rate, i.e. one star every 10^5 to 10^6 yr, as both the temperature of the disk and the gravitational tidal forces on the nascent stars are much smaller in the fermion ball than in the black hole scenario. Perhaps the stars S0-1 and S0-2, which are younger than $\sim 2 \times 10^7$ yr and have projected distances of $\lesssim$ 12 ld to the Galactic center, have been formed in this way [11]. These stars may eventually be kicked out from the central star cluster through gravitational scattering with fast moving intruder stars from the Galactic bulge or through a supernova explosion giving the supernova remnant a pulsar kick.

The formation of a degenerate fermion ball through gravitational ejection of matter, known as gravitational cooling [12], as well as the co-evolution of a fermion ball at finite temperature with an isothermal Galactic halo composed of the same fermions [13], have recently been discussed. The resulting dark matter density near the Galactic center is essentially flat, as observed, and does not exhibit the central spike predicted by cold dark matter simulations [14, 15]. As the Jeans or free-streaming mass of such collisionless fermionic matter is, with $M_{\rm FS} = 1.77\ M_{\rm Pl}^3 m^{-2} = 1.28 \times 10^{10} M_\odot$ for m = 15 keV [16], much larger than the mass of a typical dwarf galaxy ($\sim 10^8 M_\odot$), the galactic substructure in the form of dwarf galaxies will be strongly suppressed, as is apparently the case in our Galaxy, since only $\sim$ 11 dwarf galaxies are observed instead of the $\sim$ 500 predicted by cold dark matter simulations [17].

The required non-interacting fermion of $m \sim 15$ keV mass cannot be an active neutrino, as it would overclose the Universe by orders of magnitude [18]. It would also contradict the experimental upper limit on the $\nu_{\rm e}$ mass [19] and observational data on the mass squared differences between the active neutrinos, based on the oscillation interpretation of the atmospheric and solar neutrino data [20]. These data require the masses of all three active neutrinos, that are allowed by the measured Z^0 width [48], to be smaller than 2.2 eV. However, the postulated fermion could be a sterile neutrino that is very weakly mixed with at least one of the active neutrinos. Indeed, it has recently been shown [21, 22, 23] that for an acceptable primordial electron neutrino asymmetry of $\sim 10^{-2}$ or 10^{-3}, a sterile neutrino of mass $m_s \sim$ 15 keV, which is mixed with the electron neutrino at the level $\sin^2 2\theta \sim 10^{-11}$ may be produced through resonant or non-resonant scattering in the early Universe, with near closure density, i.e. $\Omega_s \sim 0.3$. The formation process which is due to mixing necessarily implies the radiative decay of the sterile neutrino into an active neutrino and a photon with a lifetime $\tau_s \sim 10^{19}$ yr, which makes this potentially unobservable dark matter particle observable. It is worth noting that the mass and the mixing angles are severely constrained by astronomical observations. First, the diffuse photon background sets the upper bounds of $m_s \lesssim 35\,\mathrm{keV}$ and $\sin^2 2\theta \lesssim 10^{-11}$ [25]. A stronger upper bound $m_s \lesssim 5\,\mathrm{keV}$ was derived [24] using the relation between the mass and the mixing angle obtained in [23]. However, if the sterile neutrino was produced resonantly [21] through a pre-existing lepton asymmetry, then the upper limit of 5 keV may be weakened substantially [24]. Futhermore, the proper inclusion of the neutrino momentum distribution sets the lower bound to $m_s \gtrsim 2.6\,\mathrm{keV}$ [26].

As an alternative possibility, the required $m \sim$ 15 keV fermion could be the axino [27] or the gravitino [28] in soft supersymmetry breaking scenarios.

2. Dynamics of the stars near the Galactic center

We now turn to a comparison of the predictions of the black hole and fermion ball scenarios of the Galactic center, for the stars with the smallest projected distances to Sgr A*, based on the measurements of their positions during the past eight years [11]. For instance, in 1996.58, seven stars (S0-1 to S0-7) were observed within a projected distance of $\sim$ 18 mpc or $\sim$ 21 ld from Sgr A*, assumed to be the dynamical center of the Galaxy. Of these seven stars, whose orbits could, in principle, contain nontrivial information on the fermion ball or black hole potentials, only three stars, S0-1 (S1), S0-2 (S2) and S0-4 (S8), show deviations from uniform motion on a straight line. For our comparative analysis, we select the star S0-2, because the independent measurements of the projected positions by Ghez *et al.* and Eckart *et al.* [11] agree very well with each other, and S0-2 would be orbiting entirely within a possible fermion ball with radius $R_c \simeq$ 21 ld.

The dynamics of the stars in the gravitational field of this nonrelativistic supermassive compact dark object can be studied solving Newton's equation of motion, taking into account the initial position and velocity vectors at, e.g., t_0 = 1992.7 yr, i.e. $\vec{r}(t_0) \equiv (x, y, z)$ and $\dot{\vec{r}}(t_0) \equiv (v_x, v_y, v_z)$. For the fermion ball, the source of the gravitational field is the mass $\mathcal{M}(r)$ enclosed within a radius r [5, 6], while for the black hole it is $M_c = \mathcal{M}(R_c)$ = 2.6 $\times$ 10$^6 M_\odot$. The mass and the degeneracy factor of the fermion are taken to be m = 16 keV and g = 2, respectively. The x-axis is chosen in the direction opposite to the right ascension (RA), the y-axis in the direction of the declination, and the z-axis points towards the sun. The black hole and the center of the fermion ball are assumed to be at the position of Sgr A*, which is also the origin of the coordinate system at an assumed distance of 8 kpc from the sun. Positions are measured in arcsec (1 arcsec = 38.8 mpc = 46.2 ld at 8 kpc distance).

There are N = 36 data points from 18 separate observations which must be fitted. The N_p = 7 free parameters are $\vec{r}(t_0)$, $\dot{\vec{r}}(t_0)$ and M_c. The χ^2 per number of degrees of freedom is defined as

$$\chi^2_{\mathrm{ndf}} = \frac{\chi^2_x + \chi^2_y}{N - N_p}\,, \tag{1}$$

with

$$\chi^2_x = \sum_{i=1}^{N} \frac{\left(x_i - \bar{x}\left(x, v_x, y, v_y, z, v_z, M_c\right)\right)^2}{\sigma^2_{x_i}}\,, \tag{2}$$

$$\chi^2_y = \sum_{i=1}^{N} \frac{\left(y_i - \bar{y}\left(x, v_x, y, v_y, z, v_z, M_c\right)\right)^2}{\sigma^2_{y_i}}\,. \tag{3}$$

The dependence of the best fit χ^2_{ndf}, as functions of v_z and z in 1992.7, are shown for both the black hole and the fermion ball scenarios in Figs. 1 and 2, respectively. The curved lines in

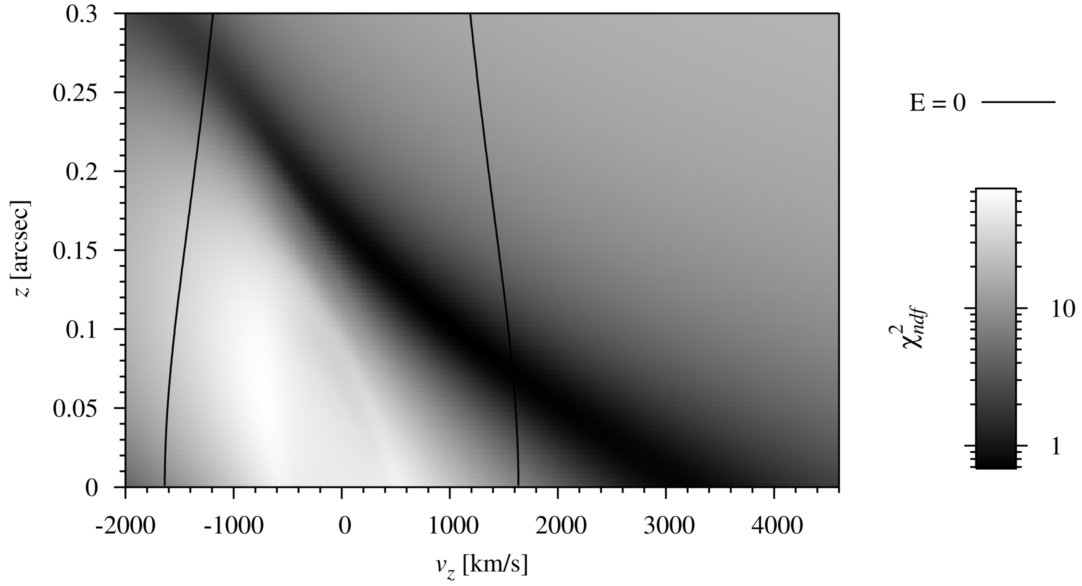

Figure 1. $\chi^2_{\rm ndf}$ phase space plot for S0-2 in the black hole scenario. Epoch 1992.7.

Figs. 1 and 2 denote a just bound orbit with a total energy $E = 0$. Thus the region within these lines describes bound orbits, while the regions outside the lines describe unbound orbits. In the absence of any gravitational scattering with stars, the orbits will be bound or nearly bound with a total energy $E \approx 0$, because the velocity dispersion at infinity is so small compared with the velocity close to the center. Thus, we believe, we should look for solutions between the curved lines in Figs. 1 and 2. The small $v_z - z$ phase space, which is allowed in the black hole scenario of Fig. 1, reflects the fact that the orbits of S0-2 depend strongly on z and v_z, while the much larger allowed $v_z - z$ phase space in the fermion ball case is due to the fact that the potential inside the fermion ball is nearly harmonic. Thus the orbits are nearly

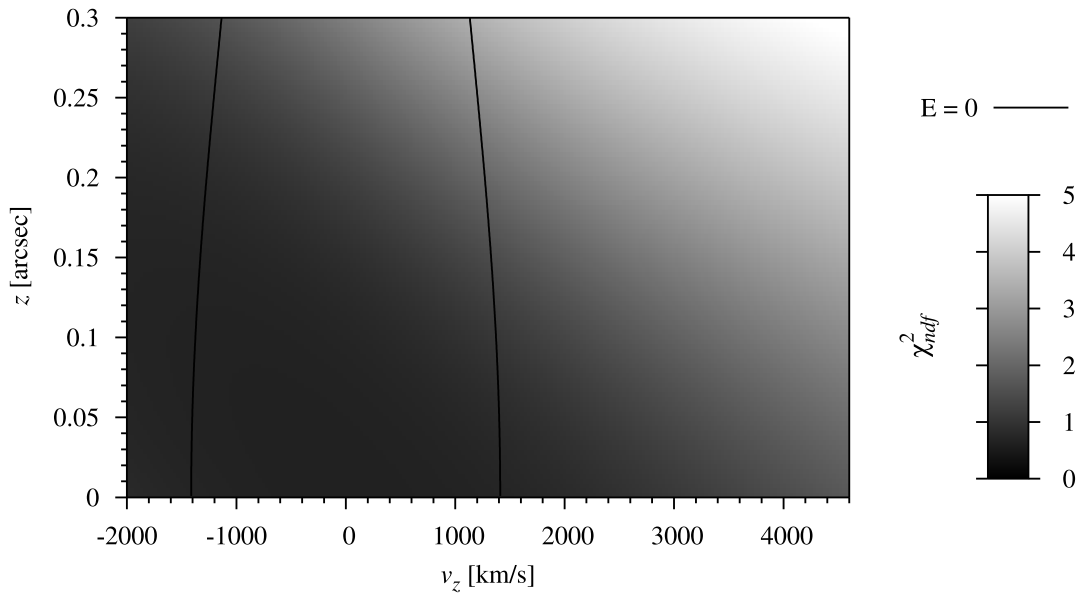

Figure 2. $\chi^2_{\rm ndf}$ phase space plot for S0-2 in the fermion ball scenario. Epoch 1992.7.

independent of z and v_z because the dynamics nearly decouples into three linear harmonic oscillators in cartesian coordinates. In Fig. 3 our best fits to the S0-2 data [11] are shown for the black hole and fermion ball scenarios. The values of the best fit parameters in 1992.7 are (x, y, z) = (- 0.028, 0.200, 0.099) arcsec and (v_x, v_y, v_z) = (300, - 300, 1090) km/sec with $\chi^2_{\rm ndf}$ = 0.68 for the black hole scenario. For the values of the best fit parameter in 1992.7 in the fermion ball case, we obtain (x, y, z) = (- 0.028, 0.200, 0.000) arcsec and (v_x, v_y, v_z) = (300, - 450, 40) km/sec with $\chi_{\rm ndf}$ = 0.65.

In Fig. 4 the orbits as they can be observed in the sky are shown for these best fits in both the black hole and fermion ball scenarios. While the bound orbits in the black hole case are closed, the bound orbits in the fermion ball scenario are open and precessing, since the potential is neither of the r^{-1} nor of the r^2 form. Of course, if the radial velocity and the coordinate, v_z and z, cannot be measured, it may take perhaps another 25 years (e.g. a half a period) to distinguish between these two scenarios. However, if some spectral lines in S0-2 could be identified, v_z may be measured via the Doppler effect. Moreover, also z could perhaps be determined by measuring the time delay

$$t_{\rm delay} = t_{\rm response} - t_{\rm flare}$$

between a particularly strong X-ray flare (assumed to originate at Sgr A*) and the perhaps observable infrared response of S0-2 through

$$z = \frac{x^2 + y^2 - c^2\, t_{\rm delay}^2}{2c\, t_{\rm delay}} \quad . \tag{4}$$

Looking at plots similar to Figs. 1 and 2, but based on the parameters of the epoch of the most recent observations, one would presumably be able to exclude one of these possible scenarios immediately if v_z and z are measured as well.

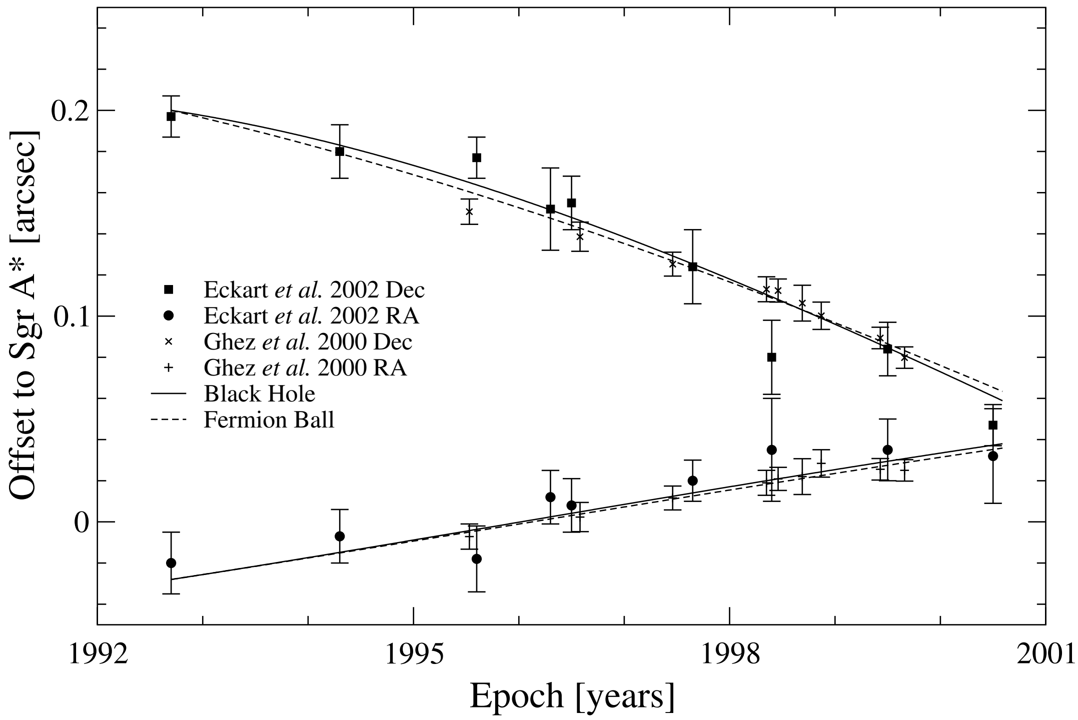

Figure 3. Best fits for S0-2. "Black Hole" denotes a bound orbit with z=0.099arcsec, v_z=1090km/s and $\chi^2_{\rm ndf} = 0.68$. "Fermion Ball" represents a bound orbit with z=0arcsec, v_z=40km/s and $\chi^2_{\rm ndf} = 0.65$.

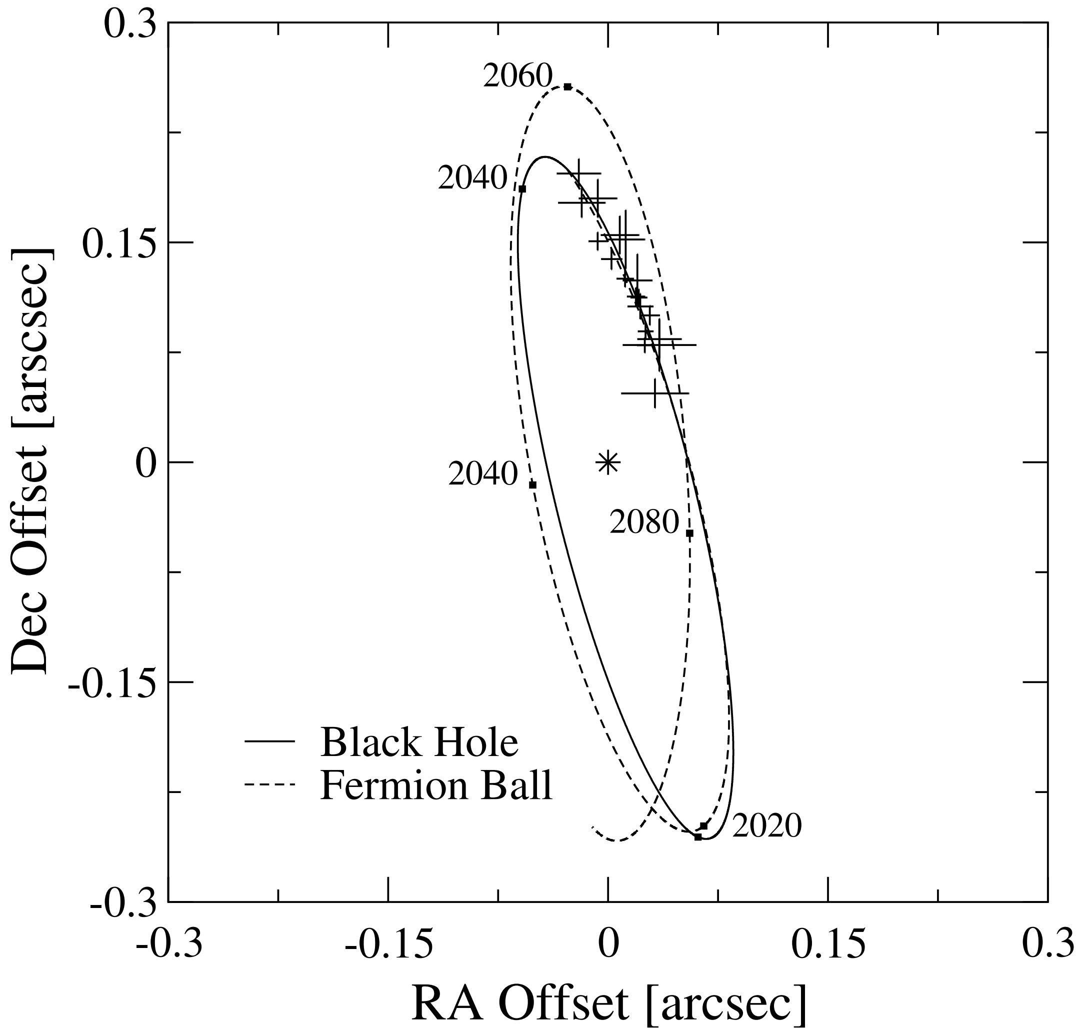

Figure 4. Best fits for S0-2, sky-plot projected until 2100. Both cases carry the same initial conditions as Fig. 3. The orbit around the black hole has a period of 50 years. The dynamic location of Sgr A* is denoted by the star.

A fermion ball at the Galactic center could also be indirectly observed through the radiative decay of the fermion (assumed here to be a sterile neutrino) into a standard neutrino, i.e. $f \to \nu\gamma$. If the lifetime for the decay $f \to \nu\gamma$ is 2.6 $\times$ 10^{19} yr, the X-ray luminosity of a M_c = 2.6 $\times$ $10^6 M_\odot$ fermion ball would be 2.8 $\times$ 10^{33} erg s^{-1}. This is consistent with the upper limit of the X-ray luminosity for the quiescent state $\sim$ 2.8 $\times$ 10^{33} erg s^{-1} of the source with radius 0.5 arcsec $\simeq$ 23 ld, whose center nearly coincides with Sgr A*, as seen by the Chandra satellite in the 2 to 7 keV band [29]. The lifetime is proportional to $\sin^{-2}\theta, \theta$ being the unknown mixing angle of the sterile with active neutrinos. With a lifetime of 2.6 $\times$ 10^{19} yr we obtain an acceptable value for the mixing angle squared θ^2 = 0.44 $\times$ 10^{-11}. The X-rays originating from such a radiative decay would contribute at least two orders of magnitude less than the observed diffuse X-ray background luminosity at this wavelength if the sterile neutrino is the dark matter particle of the Universe. The signal observed at the Galactic center would be a sharp X-ray line at $\sim$ 7.5 keV for g = 2 and $\sim$ 6.3 keV for g = 4. This line could thus be easily misinterpreted as the Fe K_α line at 6.67 keV. The X-ray luminosity would be tracing the fermion matter distribution, and it could thus be an important test of the fermion ball scenario. Of course, the angular resolution would need to be $\lesssim$ 0.1 arcsec and the sensitivity would have to extend beyond 7 keV.

In the fermion ball scenario, the $\sim$ 10 ks X-ray burst observed on 27 October 2000 near Sgr A* would have to be explained as a thermonuclear instability or runaway of material accreted or accreting on a neutron star near the center of the fermion ball. With a reasonable neutron star accretion rate of $\sim 10^{-9} M_\odot$/yr, this could also account for the strong radio emission of Sgr A* in terms of synchroton radiation due to $\sim$ 50 MeV electrons and positrons, produced in $\pi - \mu$ decays, after inelastic $N + N \to N + N + \pi$ collisions of the infalling $\sim$ 200 MeV nucleons hitting the surface of the neutron star. As accreting matter can easily spin up or slow down the rotation of neutron stars, it is perhaps also able to keep the neutron star stationary at the center of the fermion ball for an extended period of time.

In summary, it is important to note that, based on the data of the star S0-2 [11] alone, the fermion ball scenario cannot be ruled out. Similar results are obtained by analyzing the S0-1 and S0-4 data [11]. In fact, in view of the $v_z - z$ phase space, which is much larger in the fermion ball scenario than in the black hole case for both the S0-1 and S0-2 data, there is reason to treat the fermion ball scenario of the supermassive compact dark object at the center of our Galaxy with the respect it deserves.

3. Dark matter at the center and in the halo of the Galaxy

In the recent past, galactic halos were successfully modeled as a self- gravitating isothermal gas of particles of arbitrary mass, the density of which scales asymptotically as r^{-2}, yielding flat rotation curves [30]. As the supermassive compact dark objects at the galactic centers are well described by a gas of fermions of mass $m \sim 15$ keV at T = 0, it is tempting to explore the possibility that one could describe both the supermassive compact dark objects and their galactic halos in a unified way in terms of a fermion gas at finite temperature. We show here that this is indeed the case, and that the observed dark matter distribution in the Galactic halo is consistent with the existence of a supermassive compact dark object at the center of the Galaxy that has about the right mass and size.

Degenerate fermion stars are well understood in terms of the Thomas-Fermi theory applied to self-gravitating fermionic matter at T = 0 [3]. Extending this theory to nonzero temperature [31, 32, 33, 34], it has been shown that at some critical temperature $T = T_c$, a self- gravitating ideal fermion gas, having a mass below the OV limit enclosed in a sphere of radius R, may undergo a first-order gravitational phase transition from a diffuse state to a condensed state. However, this first-order phase transition can take place only if the Fermi gas is able to get rid of the large latent heat. As the short-range interactions of the fermions are negligible, the gas cannot release its latent heat; it will thus be trapped for temperatures $T < T_c$ in a thermodynamic quasi-stable supercooled state close to the point of gravothermal collapse.

The formation of a supercooled state close to the point of gravothermal collapse may be understood as the process of violent relaxation [35, 36, 37]. Through the gravitational collapse of an overdense fluctuation, $\sim$ 1 Gyr after the Big Bang, part of gravitational energy transforms into the kinetic energy of random motion of small-scale density fluctuations. The resulting virialized cloud will thus be well approximated by a gravitationally stable quasi-thermalized halo. In order to estimate the fermion mass-temperature ratio, we assume that a cold overdense cloud of the mass of the Galaxy M, stops expanding at the time $t_{\rm m}$, reaching its maximal radius $R_{\rm m}$ and minimal average density $\rho_{\rm m} = 3M/(4\pi R_{\rm m}^3)$. The total energy per fermion is just the gravitational energy

$$E = -\frac{3GM}{5\ R_{\rm m}} \ . \tag{5}$$

Assuming spherical collapse [38], one arrives at

$$\rho_{\rm m} = \frac{9\pi^2}{16}\,\bar{\rho}(t_{\rm m}) = \frac{9\pi^2}{16}\,\Omega_{\rm d}\,\rho_0\,(1+z_{\rm m})^3 \quad , \tag{6}$$

where $\bar{\rho}(t_{\rm m})$ is the background density at the time $t_{\rm m}$ or the cosmological redshift $z_{\rm m}$, and $\rho_0 \equiv 3H_0^2/(8\pi G)$ is the present critical density. We now approximate the virialized cloud by a singular isothermal sphere [39] of mass M and radius R, characterized by a constant circular velocity $\Theta = (2T/m)^{1/2}$ and the density profile $\rho(r) = \Theta^2/4\pi G r^2$. Its total energy per particle is the sum of gravitational and thermal energies, i.e.

$$E = -\frac{1}{4}\,\frac{GM}{R} = -\frac{1}{4}\,\Theta^2 \quad . \tag{7}$$

Combining Eqs. (5), (6) and (7), we find

$$\Theta^2 = \frac{6\pi}{5}\,G(6\Omega_{\rm d}\,\rho_0\,M^2)^{1/3}\,(1+z_{\rm m}) \quad . \tag{8}$$

Taking $\Omega_{\rm d}$ = 0.3, M = 2 × $10^{12} M_\odot$, $z_{\rm m}$ = 4 and H_0 = 65 km s^{-1} Mpc^{-1}, we find $\Theta \simeq$ 220 km s^{-1}, which corresponds to the mass-temperature ratio $m/T \simeq 4 \times 10^6$.

We now briefly discuss the Thomas-Fermi theory [32, 33] for a self-gravitating gas of N fermions with mass m at temperature T enclosed in a sphere of radius R. We restrict ourselves to the Newtonian theory since the general relativistic effects are not relevant to the case of our Galaxy. For large N, we can assume that fermions move in a spherically symmetric potential $\varphi(r)$ which satisfies Poisson's equation

$$\frac{d\varphi}{dr} = G\frac{\mathcal{M}}{r^2}; \qquad \frac{d\mathcal{M}}{dr} = 4\pi r^2 m n \quad , \tag{9}$$

$\mathcal{M}$ being the enclosed mass. The number density of fermions (including antifermions) n can be expressed in terms of the Fermi-Dirac distribution

$$n = \frac{\rho}{m} = g\int \frac{d^3q}{(2\pi)^3}\left(1+\exp\left(\frac{q^2}{2mT}+\frac{m}{T}\varphi-\frac{\mu}{T}\right)\right)^{-1} \quad . \tag{10}$$

Here g denotes the combined spin-degeneracy factor of neutral fermions and antifermions, i.e. g is 2 or 4 for Majorana or Dirac fermions, respectively. For each solution $\varphi(r)$ of (9), the chemical potential μ is adjusted so that the constraint

$$\int_0^R dr\, 4\pi r^2 n(r) = N \tag{11}$$

is satisfied. Equations (9) with (10) should be integrated using the boundary conditions at the origin, i.e.

$$\varphi(0) = \varphi_0; \qquad \mathcal{M}(0) = 0 \quad . \tag{12}$$

It is useful to introduce the degeneracy parameter

$$\eta = \frac{\mu}{T} - \frac{m}{T}\varphi \quad . \tag{13}$$

As φ is monotonously increasing with increasing r, the strongest degeneracy is obtained at the center with $\eta_0 = (\mu - m\varphi_0)/T$. The parameter η_0, uniquely related to the central density, will eventually be fixed by the constraint (11) or, equivalently, by the condition $\mathcal{M}(R) = mN$ at the outer boundary. In this way, the explicit dependence on the chemical potential μ is absorbed in the degeneracy parameter η_0. For $r \geq R$, the function φ yields the usual empty-space Newtonian potential

$$\varphi(r) = -G\frac{mN}{r} \quad . \tag{14}$$

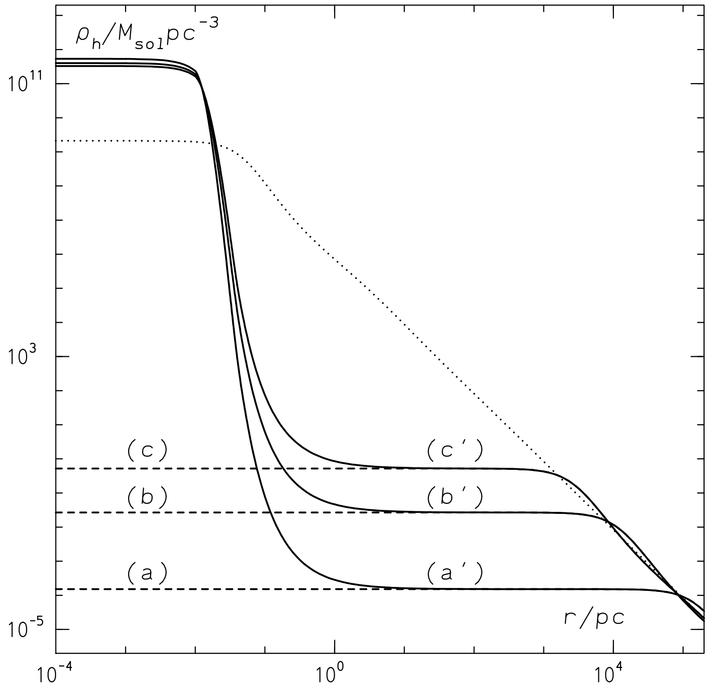

Figure 5. The mass density profile of the halo for a central degeneracy parameter $\eta_0 = 0$ (dotted line) and for the six η_0-values discussed in the text. Configurations with negative η_0 ((a), (b), (c)) are represented by the dashed and those with positive η_0 ((a'), (b'), (c')) by the solid line.

The set of self-consistency equations (9)-(11), with the boundary conditions (12), defines the gravitational Thomas-Fermi equation.

The numerical procedure is now straightforward. For a fixed, arbitrarily chosen ratio m/T, we first integrate Eqs.(9) numerically on the interval [0, R] to find the solutions for various central values η_0. This yields $\mathcal{M}(R)$ as a function of η_0. We then select the value of η_0 for which $\mathcal{M}(R) = mN$.

The quantities N, T, and R are free parameters in our model and their values are dictated by physics. In the following, N is required to be of the order $2 \times 10^{12} M_\odot/m$, so that for any m, the total mass is close to the estimated mass of the halo [40]. As we have demonstrated, the expected temperature of the halo is given by $m/T = 4 \times 10^6$. Our choice $R = 200$ kpc is based on the estimated size of the Galactic halo. The only remaining free parameter is the fermion mass, which we fix at $m = 15$ keV, justifying its choice *a posteriori*.

For fixed N, there is a range of T where the Thomas-Fermi equation has multiple solutions. For example, for $N = 2 \times 10^{12}$ and $m/T = 4 \times 10^6$, we find six solutions, which we denote by (a), (b), (c), (c'), (b') and (a'), corresponding to the values η_0 = -30.53, -25.35, -22.39, 29.28, 33.38 and 40.48, respectively. In Fig. 5 we plot the mass density profiles of the halo. For the negative central value η_0, for which the degeneracy parameter is negative everywhere, the system behaves basically as a Maxwell-Boltzmann isothermal sphere. Positive values of the central degeneracy parameter η_0 are characterized by a pronounced central core of mass of about $2.5 \times 10^6 M_\odot$ within a radius of about 20 mpc.

The presence of the core is obviously due to the degeneracy pressure. The core represents material which, having been cooled by expansion, experiences small entropy increase during the ensuing collapse. Thus the dynamics of its formation should be well approximated by a dynamical Thomas-Fermi theory based on the equation of state of a degenerate Fermi gas [12]. Conversely, the halo is formed from phase-mixed matter and estimates similar to those leading to (4) give an average entropy per particle increasing from *few* $\times$ 10^0 to *few* $\times$ 10^1.

A similar structure was obtained in collisionless stellar systems modeled as a nonrelativistic Fermi gas [41]. Note that while violent relaxation leads to a Fermi-Dirac distribution in either case, for stars the onset of degeneracy signals the breakdown of the assumption that collisions are unimportant, resulting in a Maxwell-Boltzmann distribution [36]. No such breakdown occurs for elementary fermions [37].

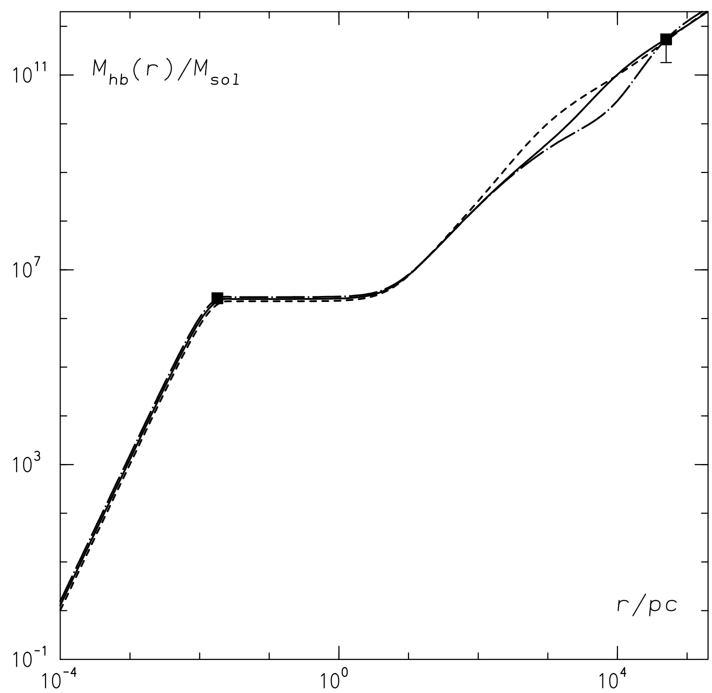

Figure 6. Enclosed mass of the halo plus bulge versus radius for η_0 = 24 (dashed), 28 (solid), and 32 (dot-dashed line).

Fig. 5 shows two important features. First, a galactic halo at a given temperature may or may not have a central core, depending on whether the central degeneracy parameter η_0 is positive or negative. Second, the closer to zero η_0 is, the smaller the radius at which the r^{-2} asymptotic behaviour of the density begins. The flattening of the Galactic rotation curve begins in the range $1 \leq r$/kpc ≤ 10, hence the solution (c') most likely describes the Galactic halo. This may be verified by calculating the rotation curves in our model. We already know from our estimate (8) that our model yields the correct asymptotic circular velocity of 220 km/s. In order to make a more realistic comparison with the observed Galactic rotation curve, we must include two additional matter components: the bulge and the disk. The bulge is

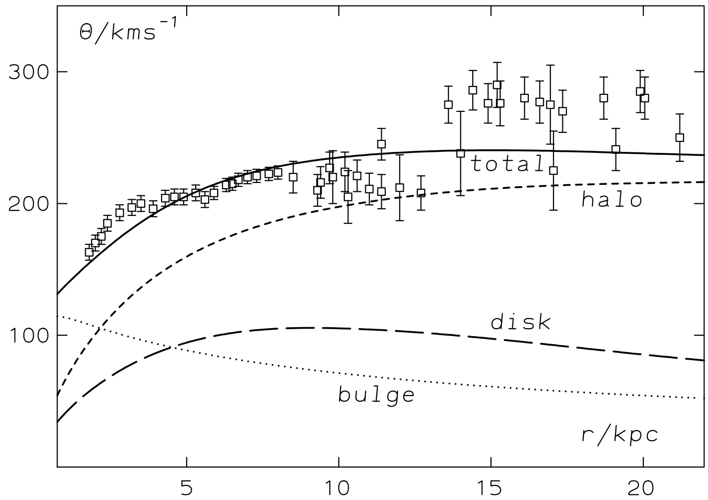

Figure 7. Fit to the Galactic rotation curve. The data points are by Olling and Merrifield [45], for $R_0 = 8.5$ kpc and $\Theta_0 = 220$ km/s.

modeled as a spherically symmetric matter distribution of the form [42]

$$\rho_{\rm b}(s) = \frac{e^{-hs}}{2s^3} \int_0^\infty du \, \frac{e^{-hsu}}{\left[(u+1)^8 - 1\right]^{1/2}} \ , \tag{15}$$

where $s = (r/r_0)^{1/4}$, r_0 is the effective radius of the bulge and h is a parameter. We adopt r_0 = 2.67 kpc and h yielding a bulge mass $M_{\rm b}$ = 1.5 × $10^{10} M_\odot$ [43]. In Fig. 6 the mass of the halo and the bulge, enclosed within a given radius is plotted for various η_0. The data points, indicated by squares, are the mass M_c = 2.6 × $10^6 M_\odot$ within 18 mpc, estimated from the motion of the stars near Sgr A* [11], and the mass M_{50} = $5.4^{+0.2}_{-3.6}$ × 10^{11} within 50 kpc, estimated from the motion of satellite galaxies and globular clusters [40]. Variation of the central degeneracy parameter η_0 between 24 and 32 does not change the essential halo features.

In Fig. 7 we plot the circular velocity components: the halo, the bulge, and the disk. The contribution of the disk is modeled as [44]

$$\Theta_{\rm d}(r)^2 = \Theta_{\rm d}(r_0)^2 \ \frac{1.97 (r/r_0)^{1.22}}{\left[(r/r_0)^2 + 0.78^2\right]^{1.43}} \ , \tag{16}$$

where we take r_0 = 13.5 kpc and $\Theta_{\rm d}$ = 100 km/s. For simplicity, here we have assumed that the disc does not influence the mass distribution of the bulge and the halo. Choosing the central degeneracy n_0 = 28 for the halo, the data by Olling and Merrifield [45] are reasonably well fitted.

We now turn to the discussion of our choice of the fermion mass m = 15 keV for the degeneracy factor g = 2. To that end, we investigate how the mass of the central object, i.e. the mass M_c within 18 mpc, depends on m in the interval 5 to 25 keV, for various η_0. We find that $m \simeq$ 15 keV always gives the maximal value of M_c ranging between 1.7 and 2.3 ×

$10^6 M_\odot$ for η_0 between 20 and 28. Hence, with $m \simeq 15$ keV we get the value closest to the mass of the central object M_c estimated from the motion of the stars near Sgr A* [11].

The radius of our central object of about 18 mpc is much larger than the size of the radio source Sgr A^*. In fact, very large array interferometric observations of Sgr A^* at millimeter wavelength show that the radiowave emitting region is $\leq$ 1-3 AU [46]. However, it has not yet been shown conclusively that Sgr A^* is indeed the object that has a mass of $\sim 3 \times 10^6 M_\odot$. There are arguments, based on the nonmotion of Sgr A^* and equipartition of energy in the central star cluster, indicating that Sgr A^* could have a mass of $\geq 10^3 M_\odot$ [47]. This argument is only conclusive if equipartition of energy actually takes place in a reasonable time frame. It is, therefore, still possible that the compact radio source Sgr A^*, with a radius of a few AU, and the moderately compact supermassive dark object that has been detected gravitationally and possibly also in X-rays in the quiescent state, with a radius of $\sim$ 20 mpc [29], could be two distinct objects.

In summary, using the Thomas-Fermi theory, we have shown that a weakly interacting self-gravitating fermionic gas at finite temperature yields a mass distribution that successfully describes both the center and the halo of the galaxy. For a fermion mass $m \simeq 15$ keV, a reasonable fit to the rotation curve is achieved with the temperature T = 3.75 meV and the degeneracy parameter at the center η_0 = 28. With the same parameters, the masses enclosed within 50 and 200 kpc are $M_{50} = 5.04 \times 10^{11} M_\odot$ and $M_{200} = 2.04 \times 10^{12} M_\odot$, respectively. These values agree quite well with the mass estimates based on the motion of satellite galaxies and globular clusters [40]. Moreover, the mass $M_c \simeq 2.27 \times 10^6 M_\odot$, enclosed within 18 mpc, agrees reasonably well with the observations of the compact dark object at the center of the galaxy. We thus conclude that both the Galactic halo and the center could be made of the same fermions.

This research is in part supported by the Foundation of Fundamental Research (FFR) grant number PHY99-01241 and the Research Committee of the University of Cape Town. The work of N.B. is supported in part by the Ministry of Science and Technology of the Republic of Croatia under Contract No. 0098002.

References

[1] M.A. Markov, Phys. Lett. **10**, 122 (1964).
[2] D. Lynden-Bell and M.J. Rees, MNRAS **152**, 461 (1971).
[3] R.D. Viollier, D. Trautmann and G.B. Tupper, Phys. Lett. B **306**, 79 (1993); R.D. Viollier, Prog. Part. Nucl. Phys. **32**, 51 (1994).
[4] N. Bilić, D. Tsiklauri and R.D. Viollier, Prog. Part. Nucl. Phys. **40**, 17 (1998); N. Bilić and R.D. Viollier, Nucl. Phys. (Proc. Suppl.) B **66**, 256 (1998).
[5] N. Bilić, F. Munyaneza and R.D. Viollier, Phys. Rev. D **59**, 024003 (1999).
[6] D. Tsiklauri and R.D. Viollier, Astropart. Phys. **12**, 199 (1999); F. Munyaneza and R.D. Viollier, astro-ph/9907318.
[7] F. Munyaneza, D. Tsiklauri and R.D. Viollier, ApJ **509**, L105 (1998); *ibid*. **526**, 744 (1999); F. Munyaneza and R.D. Viollier, ApJ **564**, 274 (2002).
[8] L.C. Ho and J. Kormendy, astro-ph/0003267; astro-ph/0003268.
[9] F. Macchetto *et al.*, ApJ **489**, 579 (1997).
[10] J.R. Oppenheimer and G.M. Volkoff, Phys. Rev. **55**, 374 (1939).
[11] A. Eckart and R. Genzel, MNRAS **284**, 576 (1997); A. Eckart, R. Genzel, T. Ott, R. Schödel, MNRAS **331**, 917 (2002); A.M. Ghez, B.L. Klein, M. Morris and E.E. Becklin, ApJ **509**, 678 (1998); A.M. Ghez, M. Morris, E.E. Becklin, A. Tanner, T. Kremenek, *Nature* **407**, 349 (2000).
[12] N. Bilić, R.J. Lindebaum, G.B. Tupper, R.D. Viollier, Phys. Lett. **B515**, 105 (2001); astro-ph/0106209.
[13] N. Bilić, G.B. Tupper and R.D. Viollier, astro-ph/0111366.
[14] B. Moore *et al.*, ApJ **499**, L5 (1998); B. Moore *et al.*, MNRAS **310**, 1147 (1999); J.F. Navarro, C.S. Frenk, S.D.M. White, ApJ **490**, 493 (1997); *ibid.* **462**, 563 (1996).
[15] P. Bode, J.P. Ostriker, N. Turok, ApJ **556**, 93 (2001).
[16] J.R. Bond, G. Efstathiou and J. Silk, Phys. Rev. Lett. **45**, 1980 (1980).

[17] B. Moore *et al.*, ApJ **524**, L19 (1999); S. Ghigna *et al.*, ApJ **544**, 616 (2000); M. Mateo, Ann. Rev. Astron. & Astrophys. **36**, 435 (1998).
[18] S.S. Gershtein and Y.B. Zeldovich, Pisma Zh. Eksp. Teor. Fiz. **4**, 174 (1966); JETP Lett. **4**, 120 (1966).
[19] C. Weinheimer *et al.*, Phys. Lett. **B460**, 219 (1999); V.M. Lobashev *et al.*, Phys. Lett. **B460**, 227 (1999).
[20] S. Fukuda *et al.*, Phys. Rev. Lett. **85**, 3999 (2000).
[21] X. Shi and G.M. Fuller, Phys. Rev. Lett. **82**, 2832 (1999).
[22] G.M. Fuller and R.A. Malaney, Phys. Rev. **D43**, 3136 (1991); E.W. Kolb and M.S. Turner, Phys. Rev. Lett. **67**, 5 (1991); G.B. Tupper, R.J. Lindebaum, and R.D. Viollier, Mod. Phys. Lett. **A15**, 1221 (2000).
[23] K. Abazajian, G.M. Fuller, and M. Patel, Phys. Rev. D **64**, 023501 (2001).
[24] K. Abazajian, G.M. Fuller, and W.H. Tucker, ApJ **562**, 593 (2001).
[25] A.D. Dolgov and S.H. Hansen, Astropart. Phys. 16, 339 (2001).
[26] S.H. Hansen, J. Lesgourgues, S. Pastor, and J. Silk, MNRAS 333, 544 (2002).
[27] T. Goto and M. Yamaguchi, Phys. Lett. B **276**, 123 (1992).
[28] D.H. Lyth, Phys. Lett. B **488**, 417 (2000).
[29] F.K. Baganoff *et al.*, astro-ph/0102151; F.K. Baganoff *et al.*, Nature **413**, 45 (2001).
[30] S. Cole and C. Lacey, MNRAS **281**, 716 (1996) and references therein.
[31] N. Bilić and R.D. Viollier, Phys. Lett. B **408**, 75 (1997).
[32] N. Bilić and R.D. Viollier, Gen. Rel. Grav. **31**, 1105 (1999).
[33] N. Bilić and R.D. Viollier, Eur. Phys. J. **C11**, 173 (1999).
[34] W. Thirring, Z. Physik **235**, 339 (1970); P. Hertel, H. Narnhofer and W. Thirring, Comm. Math. Phys. **28**, 159 (1972); J. Messer, J. Math. Phys. **22**, 2910 (1981).
[35] D. Lynden-Bell, MNRAS **136**, 101 (1967).
[36] F.H. Shu, ApJ **225**, 83 (1978); *ibid.* **316**, 502 (1987).
[37] A. Kull, R.A. Treumann and H. Böhringer, ApJ **466**, L1 (1996).
[38] T. Padmanabhan, *Structure formation in the Universe* (Cambridge University Press, Cambridge, 1993).
[39] J. Binney and S. Tremaine, *Galactic Dynamics* (Princeton University Press, Princeton, New Jersey, 1987).
[40] M.I. Wilkinson and N.W. Evans, MNRAS **310**, 645 (1999).
[41] P.-H. Chavanis and J. Sommeria, MNRAS **296**, 569 (1998).
[42] P.J. Young, ApJ **81**, 807 (1976); G. de Vaucouleurs and W.D. Pence, ApJ **83**, 1163 (1978).
[43] P.D. Sackett, ApJ **483**, 103 (1997).
[44] M. Persic, P. Salucci, and F. Stell, MNRAS **281**, 27 (1986).
[45] R.P. Olling and M.R. Merrifield, MNRAS **311**, 361 (2000).
[46] K.H. Lo *et al.*, ApJ **508**, L61 (1998).
[47] J. Zhao and W.M. Goss, ApJ **499**, L163 (1998).
[48] D.E. Grom *et al.*, Eur. Phys. J. **C15**, 1 (2000).